

# Long-lived $\pi$ edge modes of interacting and disorder-free Floquet spin chains

Daniel J. Yates<sup>1</sup>, Alexander G. Abanov<sup>2,3</sup>, and Aditi Mitra<sup>1</sup>

<sup>1</sup>*Center for Quantum Phenomena, Department of Physics,  
New York University, 726 Broadway, New York, NY, 10003, USA*

<sup>2</sup>*Simons Center for Geometry and Physics, Stony Brook, NY 11794, USA*

<sup>3</sup>*Department of Physics and Astronomy, Stony Brook University, Stony Brook, NY 11794, USA*

(Dated: May 6, 2022)

Floquet spin chains have been a venue for understanding topological states of matter that are qualitatively different from their static counterparts by, for example, hosting  $\pi$  edge modes that show stable period-doubled dynamics. However the stability of these edge modes to interactions has traditionally required the system to be many-body localized in order to suppress heating. In contrast, here we show that even in the absence of disorder, and in the presence of bulk heating,  $\pi$  edge modes are long lived. Their lifetime is extracted from exact diagonalization and is found to be non-perturbative in the interaction strength. A tunneling estimate for the lifetime is obtained by mapping the stroboscopic time-evolution to dynamics of a single particle in Krylov subspace. In this subspace, the  $\pi$  edge mode manifests as the quasi-stable edge mode of an inhomogeneous Su-Schrieffer-Heeger model whose dimerization vanishes in the bulk of the Krylov chain.

## I. INTRODUCTION

Periodically driven or Floquet systems are promising venues for identifying states of matter that do not exist in thermal equilibrium [1]. Perhaps the most striking among these athermal states are Floquet systems with new topological properties and bulk boundary correspondences that require defining new topological invariants [2, 3]. For example, while a static two-band system may be characterized by an integer  $\mathbb{Z}$  valued or a  $\mathbb{Z}_2$  valued topological invariant [4–6], two-band free fermion Floquet systems require at least one more topological invariant so that the system has a  $\mathbb{Z} \times \mathbb{Z}$  or a  $\mathbb{Z}_2 \times \mathbb{Z}_2$  classification [7–9]. The additional topological invariant arises due to the periodic nature of the Floquet spectrum. In particular, since the energy in a periodically driven system is conserved only up to integer multiples of the drive frequency  $\Omega$ , one has quasi-energy bands rather than energy bands. These quasi-energy bands span a Floquet Brillouin zone (FBZ),  $\epsilon \in [-\Omega/2, \Omega/2]$ , with the boundaries of the FBZ being continuous. The additional topological invariant characterizes edge modes that can reside at the zone boundaries  $\epsilon = \pm\Omega/2$ .

For two dimensional (2d) systems, the additional topological invariant leads to the anomalous Floquet insulator where a bulk has zero Chern number, yet chiral edge modes propagate at the boundary [10–12]. For one dimensional (1d) systems, the edge modes that reside at the Floquet zone boundary are known as  $\pi$  edge modes [13–15]. Since these modes have a periodicity which is twice that of the drive period, they are examples of boundary time crystals [16–18]. Of course, the  $\mathbb{Z} \times \mathbb{Z}$  or a  $\mathbb{Z}_2 \times \mathbb{Z}_2$  classification implies that 0 and  $\pi$  edge modes can exist separately, or together, leading to a rich phase diagram [19–22].

The  $\pi$  edge modes occurring in most 1d systems [13–15, 23] also have their origin in what are known as strong  $\pi$  modes (SPM) [24], whose precise definition we now give. Denoting the  $\pi$  strong mode as  $\Psi_\pi$ , these are operators

that have the property that they anti-commute with a discrete, say  $\mathbb{Z}_2$  symmetry, which we denote by  $\mathcal{D}$ . Thus,  $\{\Psi_\pi, \mathcal{D}\} = 0$ . In addition, the SPM anti-commutes with the Floquet unitary  $U$  that generates stroboscopic time-evolution,  $\{\Psi_\pi, U\} \approx 0$ . The symbol  $\approx$  is to represent the fact that the anti-commutation is strictly speaking obeyed only in the thermodynamic limit. For a finite size system of length  $L$ ,  $\{\Psi_\pi, U\} \propto |u|^L$ , where  $|u| < 1$ , so that the anti-commutator is suppressed exponentially in the system size. The third property that the SPM has is that it is a local operator with the property  $\Psi_\pi^2 = O(1)$ . The existence of a SPM implies an eigenspectrum phase where each eigenstate  $|n\rangle$  of a certain parity has a pair  $\Psi_\pi|n\rangle$  of the opposite parity, with the quasi-energies of the two states separated by  $\pi/T$ , where  $T = 2\pi/\Omega$  is the period of the drive. Note that the above definition of SPMs can be generalized to more complex  $2\pi/k$  edge modes where  $k$  is an integer [25].

When interactions are included, these operators no longer exactly anti-commute with  $U$  in the thermodynamic limit, and therefore acquire a lifetime. Yet a fascinating aspect of these edge modes, which is the central topic of this paper, is that the lifetime far exceeds bulk heating times [24]. These quasi-stable edge modes that almost, rather than exactly anti-commute with  $U$ , are referred to as almost strong  $\pi$  modes (ASPM). When disorder is present, leading to many-body localization, the SPM is stable to the presence of interactions at all times [19, 26–30]. This paper, in contrast, concerns the stability of  $\pi$  modes for disorder-free chains, and determines how their lifetime depends on interactions.

Note that an analogous definition exists for a strong zero mode (SZM)  $\Psi_0$  [31–34]. This is a local operator that obeys all the above properties except that  $\Psi_0$  commutes with the Floquet unitary in the thermodynamic limit  $[\Psi_0, U] \approx 0$ . Thus existence of a SZM implies an eigenspectrum phase where the entire spectrum of  $U$  is at least doubly degenerate. Adding interactions makes the SZM into a quasi-stable almost strong zero mode

(ASZM). Since SZMs and ASZMs have by now been discussed in detail in static systems [35–40], in this paper we will only focus on SPMs and ASPMs.

We will study the stroboscopic dynamics of an open spin-1/2 chain of length  $L$ . The dimension of the Hilbert space of the problem is  $2^L$ . The natural numerical method of choice is exact diagonalization (ED), and we are limited to a system size of  $L = 14$ . Since we are interested in extracting lifetimes in the thermodynamic limit of  $L \rightarrow \infty$ , ED can be restrictive, and alternate numerical and analytical methods are needed. Thus the results presented here, besides being an explication of the unusual physics of ASPMs, also provide a roadmap for developing methods for understanding slow, system size independent dynamics.

The paper is organized as follows. We first present the model and discuss its non-interacting or free limit where one obtains a SPM. Following this, we add interactions, and use ED to extract the lifetime of the ASPM. To better understand the long lifetimes, we map the dynamics of the edge operator to dynamics of a free particle in Krylov space [41]. We highlight the properties of the Krylov Hamiltonian that ensure the existence of quasi-stable edge modes despite bulk heating. We also present a tunneling argument for the long lifetime of the ASPM. We supplement this result with a domain wall counting argument based on the Floquet Hamiltonian. Finally we present our conclusions.

## II. RESULTS AND DISCUSSION

**Model:** We will study an open chain of length  $L$  whose stroboscopic time-evolution is generated by the following Floquet unitary

$$U = e^{-i\frac{T}{2}J_z H_{zz}} e^{-i\frac{T}{2}J_x H_{xx}} e^{-i\frac{T}{2}g H_z}, \quad (1)$$

where

$$H_z = \sum_{i=1}^L \sigma_i^z, \quad H_{xx} = \sum_{i=1}^{L-1} \sigma_i^x \sigma_{i+1}^x, \quad H_{zz} = \sum_{i=1}^{L-1} \sigma_i^z \sigma_{i+1}^z. \quad (2)$$

Above  $\sigma^{x,y,z}$  are the Pauli matrices, and in what follows we set  $J_x = 1$ . Eq. (1) is an example of a ternary drive where during one period, a magnetic field of strength  $Tg$  is applied, followed by the application of a nearest neighbor exchange interaction of strength  $T$  along the  $x$  direction, and this is followed by the application of a nearest neighbor exchange interaction of strength  $TJ_z$  along the  $z$ -direction. The Floquet unitary has a discrete symmetry as it commutes with  $\mathcal{D} = \sigma_1^z \dots \sigma_L^z$ .

When  $J_z = 0$ , the model can be mapped to free fermions through a Jordan-Wigner transformation. In this free limit any operator can be expanded in a basis of  $2L$  Majorana fermions or Pauli string operators. Thus when  $J_z = 0$ , the dimension of the space needed to diagonalize the problem is only  $2L$  rather than the dimension

of the full Hilbert space  $2^L$ . The existence of this free limit has been valuable for identifying strong modes. In fact, at the special point of  $Tg = \pi$ , the Floquet unitary for  $J_z = 0$  reduces to  $U = (-i)^L \mathcal{D} e^{-i\frac{T}{2}J_x H_{xx}}$  [19]. At this special point, the SPM is simply the Pauli spin operator on the first site  $\Psi_\pi = \sigma_1^x$ . It is straightforward to check that  $\sigma_1^x$  has all the properties of a SPM as summarized in the Introduction. It is a local operator with  $\Psi_\pi^2 = 1$ , it anti-commutes with  $\mathcal{D}$ , and it anti-commutes with  $U$  since  $\mathcal{D} \sigma_1^x \mathcal{D} = -\sigma_1^x$ . Even away from this special point, although the SPM is a more complex operator, it continues to have the property that it has a non-zero overlap with  $\sigma_1^x$  [14, 24].

Including interactions, i.e.  $J_z \neq 0$ , as anticipated in the Introduction, the SPM changes to an ASPM. Moreover, this operator continues to have an overlap with  $\sigma_1^x$ . Therefore, an efficient way to determine whether the system hosts these special edge modes is through the study of the following autocorrelation function

$$A_\infty(nT) = \frac{1}{2^L} \text{Tr} \left[ \sigma_1^x(nT) \sigma_1^x(0) \right], \quad (3a)$$

$$\sigma^x(nT) = [U^\dagger]^n \sigma_1^x U^n. \quad (3b)$$

We only study the dynamics at stroboscopic times, so  $n$  is an integer. Moreover,  $A_\infty$  is an infinite temperature average as the trace is over the entire Hilbert space. Thus this quantity is a highly out of equilibrium measure of the system dynamics. When an ASPM or an ASZM is non-existent or if we replace  $\sigma_1^x$  by an operator deep in the bulk of the chain,  $A_\infty$  will decay to zero within a few drive cycles. Throughout this paper, all numerical results will be for  $g = 0.3$  and  $T = 8.25$ , but for different values of  $J_z$ . For this value of  $g, T$ , when  $J_z = 0$  we have a SPM. When  $J_z$  is non-zero, the SPM changes to an ASPM.

**Exact Diagonalization (ED):** We first present results for the stroboscopic time-evolution of  $A_\infty$  from ED. Fig. 1 plots  $A_\infty$  for  $J_z = 0.01$ , for three different system sizes  $L = 6, 8, 10$ . The  $x$ -axis which denotes the stroboscopic times is on a logarithmic scale. One finds that  $A_\infty$  flips sign between neighboring stroboscopic times, thus we have an ASPM. Moreover, for small system sizes, as  $L$  increases, the lifetime of the ASPM increases (compare  $L = 6$  with  $L = 8$  in the figure), but eventually the lifetime reaches a system size independent value. For the chosen parameters, the system size independent lifetime is reached by  $L = 8$  as the plots for  $L = 8$  and  $L = 10$  nearly coincide. Moreover, for  $J_z = 0.01$ , this lifetime is around  $10^4$  drive cycles. Note that the high frequency limit requires  $T \ll 1$ , and since we have  $T = 8.25$ , we are far from the high frequency limit. Thus, the bulk is in fact heating, as expected for a periodically driven interacting, and disorder-free system [42–47]. The evidence from ED for bulk heating was already presented in Ref. 24, where it was shown that the autocorrelation function for bulk operators decays to zero within a few drive cycles, and that the entropy density rapidly

approaches the maximum possible value (accounting for finite size effects). Further below, we will discuss the signature of bulk heating in Krylov subspace.

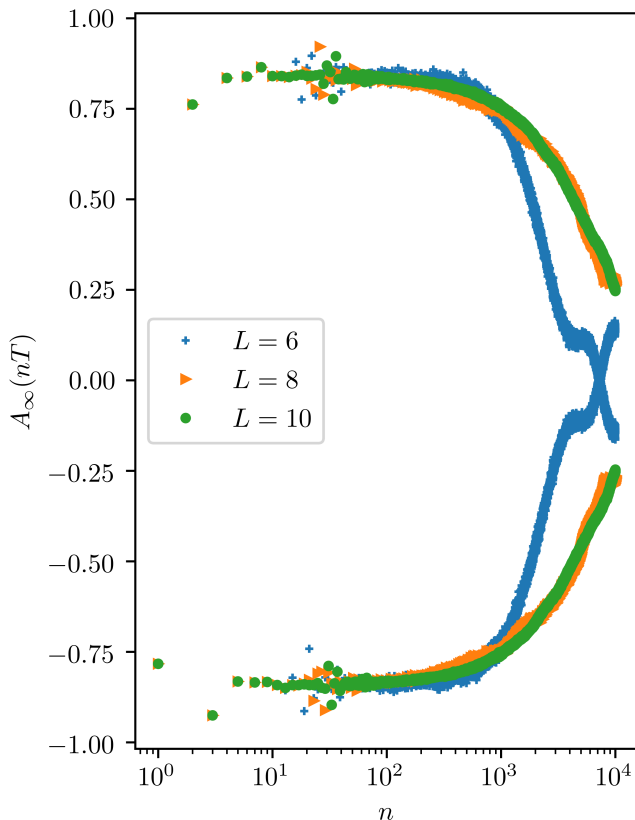


FIG. 1.  $A_\infty$  at stroboscopic times for  $g = 0.3$ ,  $J_z = 0.01$ , and  $T = 8.25$ , for three different system sizes  $L = 6, 8, 10$ . The  $x$ -axis is on a logarithmic scale. The system hosts an ASPM as is clearly visible by the flipping of the sign of  $A_\infty$  between neighboring stroboscopic times. For this choice of parameters, the thermodynamic limit is already reached for  $L = 8$  as the decay time for the ASPM is the same for  $L = 8$  and  $L = 10$ . This decay time is approximately  $10^4$  drive cycles.

We now discuss how the lifetime in the thermodynamic limit depends on  $J_z$ . Fig. 2 shows the autocorrelation function accounting for its period-doubled behavior  $A_\infty^p(nT) = (-1)^n A_\infty(nT)$ . Since the sign-flipping of  $A_\infty$  is absorbed by the  $(-1)^n$  factor,  $A_\infty^p$  has a smoother behavior in time. We plot  $A_\infty^p$  for different  $J_z$  and for system sizes  $L = 8, 10, 12, 14$ . The smallest possible  $J_z$  we can study is  $J_z = 0.001$  because for  $J_z$  values smaller than this, the system size needed for the lifetime to become  $L$  independent, is larger than  $L = 14$ . While the stroboscopic times in Fig. 1 were linearly separated, the stroboscopic times in Fig. 2 are logarithmically separated as the lifetimes increase dramatically with decreasing  $J_z$ , and linearly separated points are numerically too costly to compute.

Fig. 2 clearly shows that as  $J_z$  increases (top to bottom panels), the lifetime of the ASPM decreases. In fact the

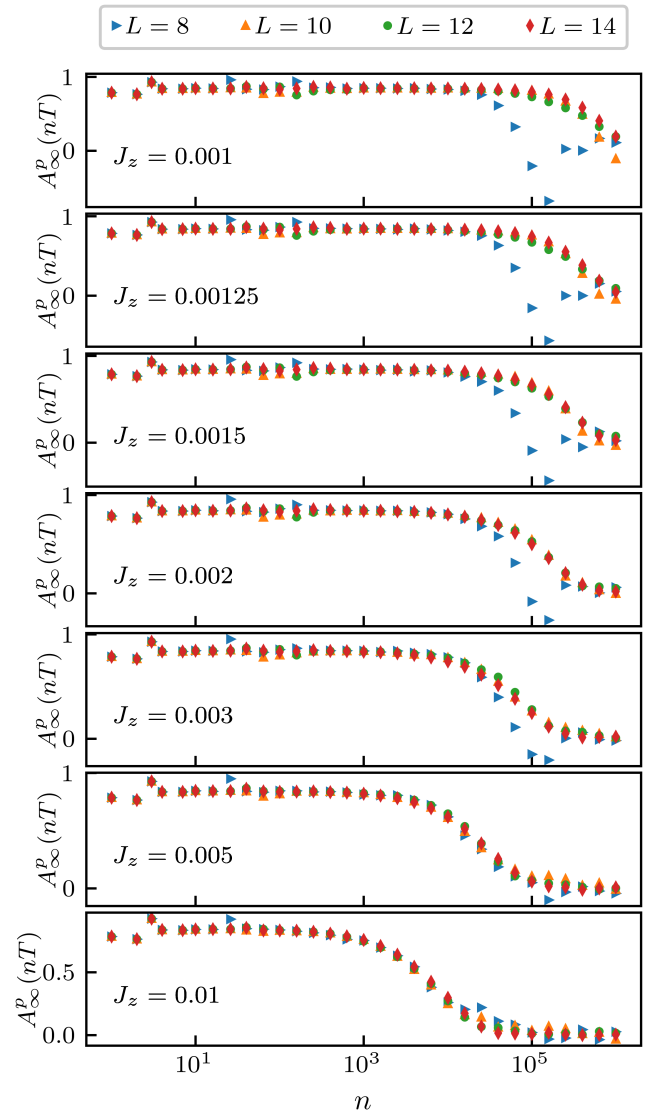


FIG. 2.  $A_\infty^p(nT) = (-1)^n A_\infty(nT)$  at stroboscopic and logarithmically separated times for  $g = 0.3$ ,  $T = 8.25$  and different  $J_z$ . The  $x$ -axis is on a logarithmic scale. From top to bottom panel,  $J_z$  increases. The lowest panel corresponds to  $J_z = 0.01$  and the corresponding time evolution for  $A_\infty(nT)$  for linearly separated times is shown in Fig. 1.

thermodynamic lifetimes are already reached for  $L = 8$  when  $J_z = 0.01$  as the plots for all the four system sizes lie on top of each other (lowest panel). Recall that Fig. 1 is a more detailed version of  $A_\infty$  for precisely this value of  $J_z$ , where the stroboscopic times are linearly separated, and one smaller system size,  $L = 6$ , is shown in order to highlight the system size dependence.

By employing an ansatz that  $A_\infty(nT) \approx e^{-\Gamma(n-1)T} A_\infty(T)$ , the decay rate  $\Gamma$  is extracted from determining the time at which  $A_\infty(\Gamma^{-1}) \approx e^{-1} A_\infty(T)$ . The decay rates obtained from this definition are plotted in Fig. 3 where now it is the  $y$ -axis that is plotted on a

logarithmic scale. The almost linear slope for  $1/J_z \gg 1$  suggests that (restoring  $J_x$ )

$$\Gamma \sim e^{-cJ_x/J_z}. \quad (4)$$

Above  $c$  is a  $O(1)$  number that depends on  $g, J_x$ . Thus for small enough  $J_z$ , ED indicates that the decay rates are non-perturbative in the strength of the interactions  $J_z$ . As  $J_z$  is further increased, we do not expect the edge mode to be an ASPM, and its decay rate will be determined entirely by perturbative processes  $\Gamma \propto O(J_z^\alpha)$ , where  $\alpha$  is a power of  $O(1)$ .

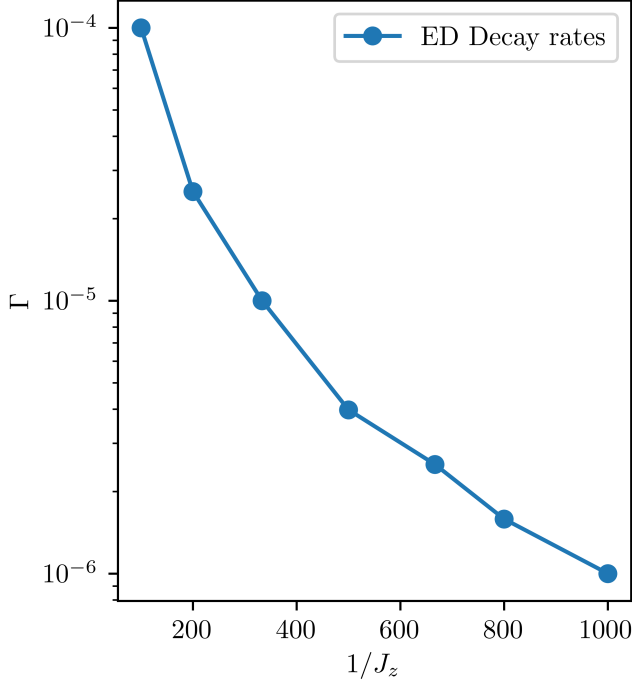


FIG. 3. The decay rate from the ED data in Fig. 2 plotted on a logarithmic scale vs  $1/J_z$ . The linear slope at  $1/J_z \gg 1$  indicates that  $\Gamma \approx e^{-c/J_z}$  where  $J_z$  is in units of  $J_x$  and  $c$  is a  $O(1)$  number.

**Krylov subspace dynamics:** In order to understand the origin of the non-perturbatively long lifetimes for  $J_z \ll 1$ , and its relation to bulk heating, we map the stroboscopic time-evolution of  $\sigma_1^x$  to dynamics of a free particle in a Krylov subspace employing a recursive Lanczos scheme [41, 48–51]. This mapping to single particle physics will allow us to develop a tunneling picture for the lifetime of the ASPM.

Let us define the Floquet Hamiltonian as  $H_F = i \log(U)/T$ . The stroboscopic time-evolution after  $m$  periods of a Hermitian operator  $O$  can be written in terms of  $H_F$  as follows

$$[U^\dagger]^m O U^m = e^{iH_F mT} O e^{-iH_F mT} = \sum_{n=0}^{\infty} \frac{(imT)^n}{n!} \mathcal{L}^n O, \quad (5)$$

where we define  $\mathcal{L}O = [H_F, O]$ . To employ the Lanczos algorithm, we recast the operator dynamics into vector dynamics by defining  $|O\rangle = O$ . Since we are concerned with infinite temperature quantities, we have an unambiguous choice for an inner product on the level of the operators,  $\langle A|B\rangle = \text{Tr}[A^\dagger B]/2^L$ . The Lanczos algorithm iteratively finds the operator basis that tri-diagonalizes  $\mathcal{L}$ .

We begin with the seed “state”,  $|O_1\rangle$ , and let  $\mathcal{L}|O_1\rangle = b_1|O_2\rangle$ , where  $b_1 = \sqrt{|\mathcal{L}|O_1|^2}$ . The recursive definition for the basis operators  $|O_{n \geq 2}\rangle$  is,  $\mathcal{L}|O_n\rangle = b_n|O_{n+1}\rangle + b_{n-1}|O_{n-1}\rangle$ , where we define  $b_n = \sqrt{|\mathcal{L}|O_n|^2}$ . It is straightforward algebra to check that the above procedure will yield a  $\mathcal{L}$  of the form

$$\mathcal{L} = \begin{pmatrix} & b_1 & & \\ b_1 & & b_2 & \\ & b_2 & & \ddots \\ & & \ddots & \end{pmatrix}. \quad (6)$$

The basis spanned by  $|O_n\rangle$  lies within the Krylov subspace of  $\mathcal{L}$  and  $|O_1\rangle$ . We refer to this tri-diagonal matrix as the Krylov Hamiltonian  $H_K$ ,  $H_K = \sum_n b_n(c_n^\dagger c_{n+1} + c_{n+1}^\dagger c_n)$ , and the 1d lattice it represents, as the Krylov chain.

For free systems, the operation  $\mathcal{L}|O_n\rangle$  can be efficiently solved in the Majorana basis. If the starting operator is a single Majorana, then the dimension of the Krylov subspace of that operator will scale as  $2L$ , as free system dynamics can only mix the individual Majoranas among themselves. Outside of free problems, the size of the full set of  $|O_n\rangle$  will be large. For example, a system of size  $L$  will have  $\sim 2^{2L}$  possible basis operators. Since we are interested in the thermodynamic limit, in what follows, we will treat the Krylov chain to be a semi-infinite chain. The Krylov chain of interest to us is the one where the seed operator  $|O_1\rangle = |\sigma_1^x\rangle$ . Then  $A_\infty$  is equivalent to  $A_\infty(nT) = (e^{i\mathcal{L}nT})_{1,1}$ . Thus following the above discussion, the dynamics of  $A_\infty$  has been transformed into that of a semi-infinite, single-particle problem where  $A_\infty(nT)$  is now the probability that a particle initially localized at the end of the Krylov chain, stays localized at the end at time  $nT$ .

As a point of orientation, let us discuss the details of the Krylov subspace in the free limit. In the Majorana basis, the stroboscopic time evolution of  $\sigma_1^x = a_1$  is

$$U^\dagger a_1 U = K[a_1, a_2, \dots, a_{2L}]^T, \quad (7)$$

where  $K$  is a  $2L \times 2L$  matrix and the  $a_i$  are Majorana fermions. The components of  $K$  can be determined analytically [14, 24]. On comparing equations (5) and (7), we identify the operator  $O$  with  $a_1$ , and the operator  $iT\mathcal{L}$  with  $\ln K$ . Since  $\mathcal{L}$  is an operator, whose precise form depends on the basis, we have argued that  $H_K$  is related to  $i \ln K$  by a simple basis rotation.

The form of  $i \ln K$  becomes particularly simple close to the exactly solvable point  $gT = \pi$  and in the high

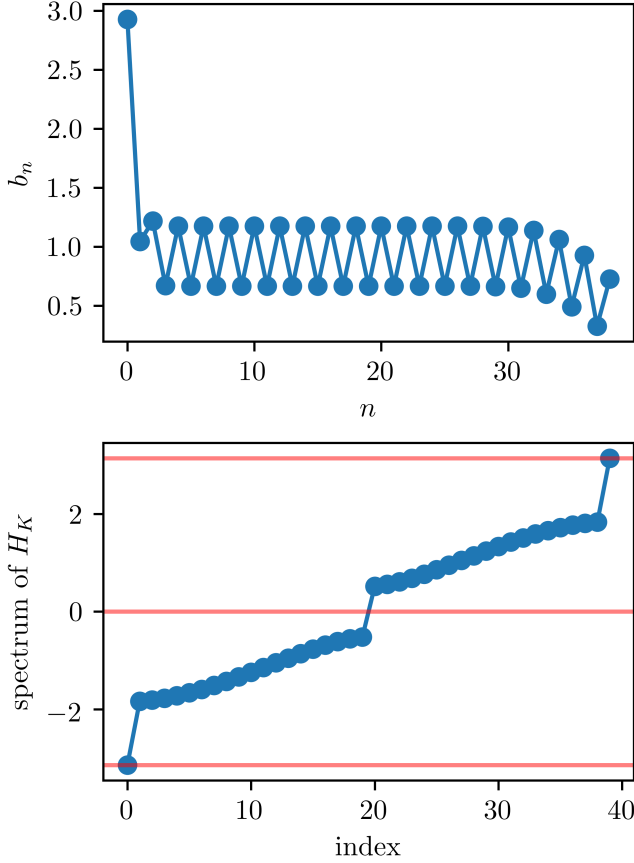


FIG. 4. The hopping parameters  $b_n$  for the Krylov chain (top panel) and the corresponding spectrum (bottom panel) for the free case ( $J_z = 0$ ) and with  $g = 0.3$ ,  $T = 8.25$  and  $L = 20$ . The horizontal red lines in the bottom panel indicate energies at  $0, \pm\pi$ . The figure shows modes at  $\pm\pi$  that are clearly separated from bulk states by an energy gap.

frequency limit  $T \ll 1$ . Denoting  $s_1 = |\pi - gT|$ , in the first order in  $s_1$  and  $T$  we find

$$i \ln K \approx \begin{pmatrix} 0 & is_1 & 0 & 0 & 0 & 0 \\ -is_1 & 0 & -iT & 0 & 0 & 0 \\ 0 & iT & 0 & is_1 & 0 & 0 \\ 0 & 0 & -is_1 & 0 & -iT & 0 \\ 0 & 0 & 0 & iT & 0 & is_1 \\ 0 & 0 & 0 & 0 & -is_1 & 0 \end{pmatrix} \pm \pi. \quad (8)$$

The above expression was obtained by first writing  $K = K_0 + V$  where  $K_0 = K(gT = \pi)$  and  $V = O(s_1)$ . If  $T \ll 1$  then the commutator of  $K_0$  and  $V$  is  $O(s_1 T) \ll 1$ .  $K_0$  and  $V$  commute if one neglects terms of  $O(s_1 T)$  and higher, and we can use  $\ln(K_0 + V) \approx \ln K_0 + K_0^{-1}V + \dots$  to derive Eq. (8). The analytic result in Eq. (8) shows that  $i \ln K$  is like a Su-Schrieffer-Heeger (SSH) model with a topologically non-trivial dimerization for  $|s_1| < T$ . Moreover the overall shift of  $\pi$  ensures that the edge mode of the SSH model is pinned at  $\pi$  rather than at zero en-

ergy.

The  $b_n$ s for  $g = 0.3$  and  $T = 8.25$ , and for the free case  $J_z = 0$  are shown in the top panel of Fig. 4. For this case,  $|gT - \pi|$  and  $T$  are no longer small. The bottom panel shows the corresponding spectrum of the Krylov chain, where the three horizontal red lines are at  $\epsilon = 0, \pm\pi$ . One finds that, as suggested by the analytic form in Eq. (8), the chain is a SSH model with a uniform dimerization after  $n \gtrsim 4$ . Moreover, the hopping on the very first site is large. The reason for this can be traced back to the first Lanczos step which takes  $|a_1\rangle$  and changes its “norm” to  $\pi$ , in addition to generating an orthogonal state  $|a_2\rangle$  with amplitude  $O(s_1)$ .  $b_1$  measures the norm of this new state, and therefore  $b_1 = \pi + O(s_1)$ . This initial large hopping in the Krylov chain ensures that the edge modes of the SSH model are pinned at  $\pm\pi$ , as shown in the lower panel of Fig. 4. In fact the effective model for the Krylov chain for  $J_z = 0$  can be written as  $H_K = H_{\text{SSH}} + H_E$ , where  $H_{\text{SSH}}$  represents a SSH model and captures the behavior from sites  $n \gtrsim 4$ , while  $H_E$  is an edge Hamiltonian that captures the physics on the first few sites. The SPM  $\psi_\pi$  is a zero mode of  $H_{\text{SSH}}$ , while  $H_E \psi_\pi = \pi \psi_\pi$ . Thus  $H_K \psi_\pi = \pi \psi_\pi$ . To obtain a  $\pi$  edge mode, the parameters of  $H_E$  are finely tuned, while  $H_{\text{SSH}}$  only requires its dimerization to be topologically non-trivial to ensure a zero mode. The role of  $H_E$  is to raise the energy of the zero mode to  $\pi$ .

Note that this mapping from the Floquet unitary  $U$  to the Krylov chain has lost information about the periodic nature of the spectrum of  $U$ , and this manifests as finely tuned  $b_n$  at the edge of the Krylov chain when a  $\pi$  mode exists. Nevertheless this mapping to an effectively free model helps to arrive at a tunneling estimate for the lifetime of the  $\pi$  mode when interactions are non-zero. We discuss this below.

We now switch on interactions. We expect the dynamics to explore larger regions of the Hilbert space, resulting in more complicated  $b_n$ . These are shown in the upper panel of Fig. 5 for system size  $L = 12$  and with different  $J_z$ . The lower panel shows the corresponding spectra. For easy comparison between the free and interacting cases, the first upper and lower panels correspond to  $J_z = 0$ . The blue dots correspond to carrying out the Lanczos procedure in the spin basis, which is the natural choice when interactions are present. In contrast, the free case involved performing Lanczos in the Majorana basis. The periodicity of  $U$  is lost in the Lanczos approach, and the resulting  $b_n$  are sensitive to the choice of the branch of  $\ln(U)$ . This leads to  $b_n$ s, shown in blue, which do not bear much of a resemblance to the  $b_n$ s of the free case, making them harder to interpret. The corresponding spectra are also shown in blue in the lower panel, and now these spectra are not restricted to the FBZ. One may map the dynamics to an alternate Krylov subspace using an Arnoldi iteration scheme [52] that works directly with the Floquet unitary, rather than its logarithm, and therefore bypasses some of the ambiguities of the Lanczos iteration. Alternatively, below we devise a scheme

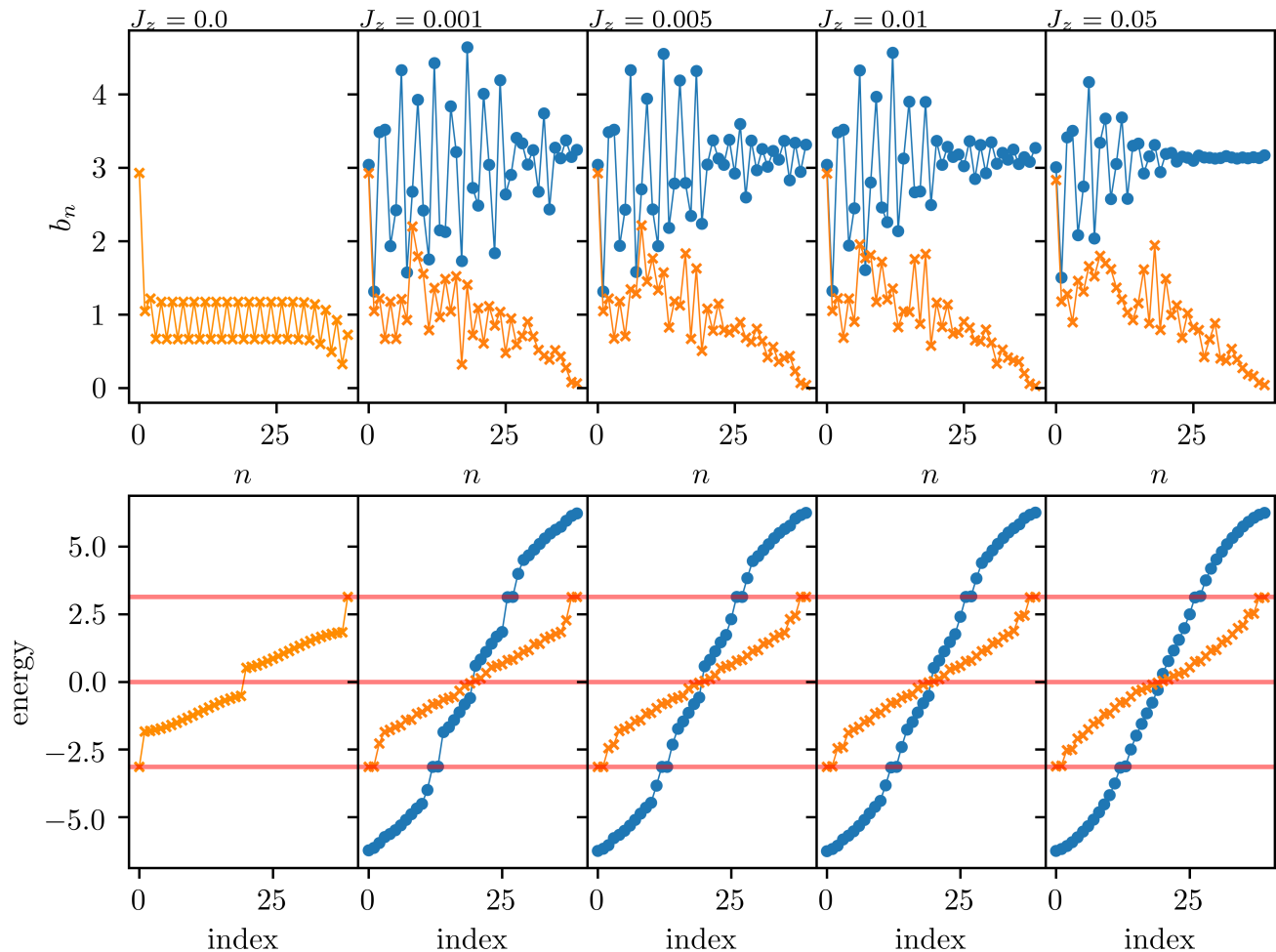


FIG. 5. The Krylov chain hopping parameters  $b_n$  (upper panels) and the corresponding spectra (lower panels) for  $g = 0.3$ ,  $T = 8.25$ , and for  $J_z$  increasing from left to right, with  $J_z = 0$  shown in the first panels. The system size for  $J_z = 0$  is  $L = 20$  (same as Fig. 4), while that for the interacting cases is  $L = 12$ . Blue circles are for the unfolded spectra, while orange crosses for non-zero  $J_z$ s are for a gauge choice where the spectra have been folded back into the FBZ. The folded spectra, and the corresponding  $b_n$  bear a closer resemblance to the free problem. The horizontal red lines in the bottom panels indicate energies at  $0, \pm\pi$ .

that can extract the relevant physics from Lanczos by a suitable gauge choice.

Since the spectra are periodic, a physically more suitable gauge choice for the Krylov Hamiltonian is the one where the spectra are folded back to lie within the FBZ (orange data in the lower panels in Fig. 5). This folding requires transforming the Krylov Hamiltonian  $H_K \rightarrow U_K \hat{\epsilon}_{\text{FBZ}} U_K^\dagger$ , where  $\hat{\epsilon}_{\text{FBZ}}$  is a diagonal matrix where all the energies lie in the FBZ, and  $U_K$  is the unitary matrix that diagonalizes  $H_K$  before the folding. The folding procedure is non-local, and therefore gives a new Hamiltonian, which is no longer tri-diagonal. Therefore, a second Lanczos iteration is carried out to recover the tri-diagonal form, resulting in a new set of  $b_n$ s that are shown in orange in the upper panels for  $J_z \neq 0$ . After this transformation, the new  $b_n$ s bear a closer resemblance to the  $b_n$ s of the free case, thus making them easier to in-

terpret.

In comparison to the free case, one notices that a dimerization persists even with interactions, but is non-uniform, and gradually decreases into the bulk of the chain. This is visible in both gauges, i.e., blue and orange data on the top panels of Fig. 5. The larger  $J_z$  is, the more rapidly the dimerization decays into the chain. The contrast is most visible between the second panel with  $J_z = 0.001$  and the last panel with  $J_z = 0.05$ . The region of the chain where there is no dimerization, represents a metallic state. Thus we have a spatially inhomogeneous system in the presence of  $J_z$  where a disordered insulating region (represented by spatially fluctuating dimerization) is separated from a metallic bulk. An operator with weight in the metallic bulk will spread rapidly, and its autocorrelation function will decay to zero within a few drive cycles. The existence of the metal is the signature



of bulk heating. Recall that for the free case the dimerization exists throughout the bulk. Thus the structure of the  $b_n$ s for  $J_z \neq 0$  gives us evidence that a quasi-localized edge mode can exist despite bulk heating.

The above picture also clarifies how the ASPM acquires a lifetime. Essentially the edge mode is localized initially at the left end of the chain, and is separated by a finite region of dimerization from the metallic bulk. Therefore, it has a non-zero probability of tunneling into the metallic region. Below we estimate the lifetime of the ASPM by determining this tunneling probability.

In order to make the discussion more quantitative, in the upper panel of Fig. 6 we plot the absolute value of the nearest-neighbor  $b_n$ s corresponding to the orange data of Fig. 5,  $M(n) = b_{n+1} - b_n$ , after performing a moving average over 4 sites. Denoting this quantity as  $\langle |M(n)| \rangle_4$ , we note that it does not change with  $J_z$  for the first couple of sites (provided  $J_z < 0.05$ ), while away from the edge,  $\langle |M(n)| \rangle_4$  decreases with  $n$  when  $J_z \neq 0$ . In contrast,  $\langle |M(n)| \rangle_4$  stays constant for the free case. The fact that the first few sites of the Krylov chain do not change with  $J_z$  implies that  $H_E$  is not sensitive to  $J_z$ . We therefore adopt a simple model of a Krylov chain for the sites  $n \gtrsim 4$ , with two slowly varying parameters, a nearest-neighbor average hopping  $(b_n + b_{n-1})/2$ , and the dimerization  $M(n)$  [39, 40]. We derive a continuum model under the assumption that the nearest-neighbor average hopping is spatially uniform, and that the dimerization is slowly varying in space. These assumptions map the Krylov chain onto a Dirac model with a spatially inhomogeneous mass [40]  $i\partial_t \tilde{\Psi} = [m(x)\sigma^y + \sigma^x i\partial_x] \tilde{\Psi}$ , where  $m(n) = M(2n)$ . For  $J_z = 0$ , the mass is spatially uniform and topologically non-trivial,  $m > 0$ , with  $M(2n) = -M(2n+1) = m$ . For  $J_z \neq 0$ , this mass vanishes into the bulk. While the precise model for how it vanishes is complicated, we adopt a simple ansatz where  $m(x) = M_0\theta(x - X_0)$ . Then a WKB treatment shows that the lifetime of the edge mode is [40]  $\Gamma \approx 4M_0e^{-2M_0X_0}$ . The fact that the edge mode is at  $\pi$  energy rather than at zero energy enters in the boundary condition via  $H_E$ , where a strong local hopping pins the edge mode to  $\pi$ .

We now discuss the  $J_z$  dependence of  $M_0$ . The lower panel of Fig. 6 shows that  $\langle |M(n=24)| \rangle_4 \sim J_z^{-1}$ . Since the decay-rate  $\Gamma$  depends on the mass  $M_0$  exponentially, and  $M_0 \propto 1/J_z$ , we conclude that  $\Gamma \sim e^{-c/J_z}$ .

**Bound for lifetime from domain wall counting argument:** We now present an alternate argument for the non-perturbatively long lifetime in Eq. (4). We show below that despite the low frequency driving, the energy required to flip the spin on the very first site is highly off resonant, and requires rearranging many domain walls in the bulk. This phenomena was also noted in previous studies on static systems [35, 38, 39, 53]. Thus the boundary is in a prethermal state [54–58], despite the

thermalized bulk. We argue this physics by deriving a Floquet Hamiltonian  $H_F$  in the limit of  $J_z \ll 1$  and  $|qT - \pi| \ll 1$ . Recall  $qT = \pi$  and  $J_z = 0$  is the exactly

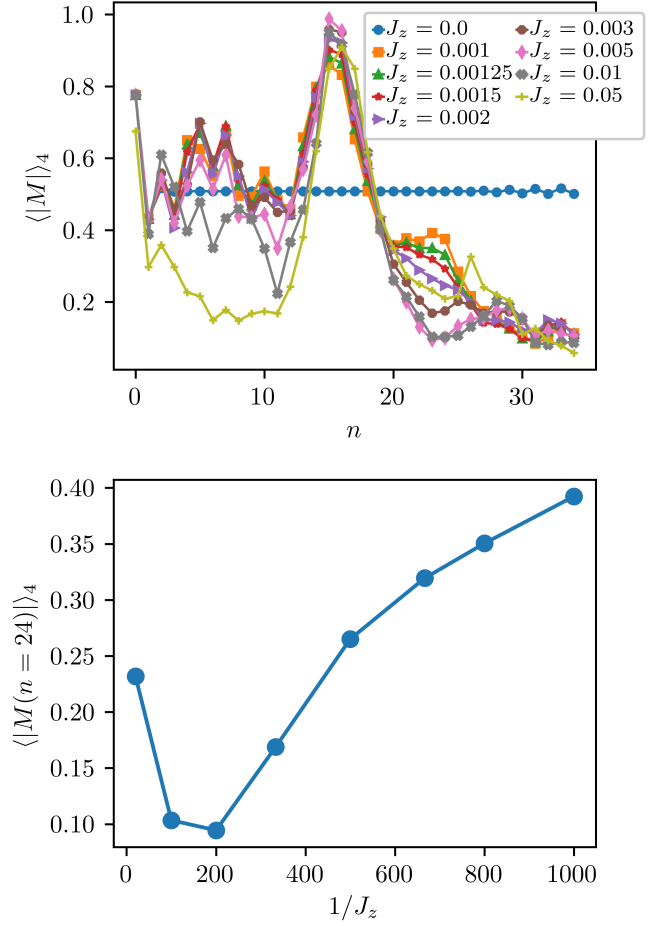


FIG. 6. The plot of the absolute value of the difference between neighboring  $b_n$ s,  $M(n) = b_{n+1} - b_n$ , after a moving average over four sites, and denoted as  $\langle |M| \rangle_4$ . Upper panel shows how this quantity varies with  $n$  as well as  $J_z$ . Lower panel shows the variation with  $1/J_z$  for this quantity at  $n = 24$ . The lower panel indicates that the dimerization decays with interactions as  $\langle |M(n=24)| \rangle_4 \propto 1/J_z$  for  $1/J_z \gg 1$ .

solvable limit where the SPM is  $\Psi_\pi = \sigma_1^x$ .

Let us define  $\hat{J}_z = J_z T/2$ ,  $\hat{g} = Tg/2 - \pi/2$  and  $\hat{J}_x = TJ_x/2$ . We will work in the limit  $\hat{J}_x \gg 1$  and  $\hat{J}_z, \hat{g} \ll 1$ . We cannot perform a high-frequency expansion [59] to construct  $H_F$  as  $\hat{J}_x$  is not small. Nevertheless,  $H_F$  to first order in  $\hat{J}_z, \hat{g}$  but to arbitrary orders in  $\hat{J}_x$  may be derived from an infinite resummation of the Baker-Campbell-Hausdorff formula [60, 61], leading to the following non-local perturbed Ising model [24]

$$\begin{aligned}
TH_F \approx & \hat{J}_x H_{xx} + \frac{\pi}{2} \mathcal{D} + \hat{g} \left\{ h_z^E \hat{J}_x \cot(\hat{J}_x) + h_z^B \left( \frac{1 + 2\hat{J}_x \cot(2\hat{J}_x)}{2} \right) + h_{zx} \left( \frac{-1 + 2\hat{J}_x \cot(2\hat{J}_x)}{2} \right) - \hat{J}_x (h_{xy} + h_{yx}) \right\} \\
& + \hat{J}_z \left\{ h_{zz}^E \hat{J}_x \cot(\hat{J}_x) + h_{zz}^B \left( \frac{1 + 2\hat{J}_x \cot(2\hat{J}_x)}{2} \right) - h_{xyx} \left( \frac{-1 + 2\hat{J}_x \cot(2\hat{J}_x)}{2} \right) + \hat{J}_x (h_{zyx} + h_{xyz}) \right\} + O(\hat{g}^2, \hat{J}_z^2).
\end{aligned} \tag{9}$$

Above  $h_{\alpha_1 \dots \alpha_k} = \sum_j \sigma_j^{\alpha_1} \dots \sigma_{j+k-1}^{\alpha_k} \equiv h_{\alpha_1 \dots \alpha_k}^E + h_{\alpha_1 \dots \alpha_k}^B$ , where  $h^E$  denotes the contributions from the edge spins  $\sigma_{1,L}^\alpha$  and  $h^B$  denotes the bulk spins.

Let us consider the energetics involved in flipping  $\sigma_1^x$  for  $\hat{g} = \hat{J}_z = 0$ . Since the boundary spin has only one neighbor, this flip costs energy  $\hat{J}_x$ . However, the energy cost for creating a domain wall in the bulk is  $2\hat{J}_x$  due to the two neighboring sites. Thus there is a mismatch of  $\hat{J}_x \gg 1$  between a bulk and an edge excitation, making the flipping of an edge spin impossible. However this simple argument does not account for processes that can make the domain wall hop from site to site, resulting in a lowering of its energy. Thus, we have to revisit the energy argument by accounting for the kinetic energy of the domain walls.

In order to develop our argument, we first note that  $H_{xx}$  counts the number of domain-walls  $N = \sum_i \sigma_i^x \sigma_{i+1}^x$ . Therefore, we write  $H_F$  as a part that commutes with the number of domain walls, and a part that changes the number of domain walls. In particular,  $TH_F = \hat{J}_x N + D + V$  where  $[D, N] = 0$  and  $[V, N] \neq 0$ . Both  $D$  and  $V$  can be written in the form similar to Eq. (9), i.e., as sums over local strings of Pauli matrices. The precise forms of  $D$  and  $V$  are not needed for our qualitative argument. We only assume that the operator norms of each of the local terms of  $D$  and  $V$  are  $O(\hat{g}, \hat{J}_z)$ . If these assumptions are valid we can apply the arguments of Refs. [35, 38, 39, 53] to find a lower bound on the lifetime of the ASPM. Here, we briefly summarize the physical picture.

First, consider the Hamiltonian  $\hat{J}_x N + D$ . The spectrum of the  $\hat{J}_x$ -term are states that are separated by multiples of  $\hat{J}_x$  because  $N$  counts domain walls. The  $D$ -term causes the domain walls to move without changing their number. Diagonalization of  $\hat{J}_x N + D$  results in domain wall “bands” with a typical bandwidth  $\epsilon \sim \|D\| \sim O(\hat{g}, \hat{J}_z)$  which is much smaller than the separation  $\hat{J}_x$  between the bands.

The  $V$ -term of the total Hamiltonian does change the number of domain walls, but only by an even number due to the parity symmetry of the total Hamiltonian. A single application of  $V$  therefore changes the energy by about  $2\hat{J}_x$  and is off resonant with the cost  $\hat{J}_x$  of flipping the boundary spin. It is impossible to absorb the energy  $\hat{J}_x$  within few orders of perturbation theory in  $V$ . However, the creation and annihilation of a pair of domain walls would lead to the change of the energy by the order of the bandwidth  $\epsilon \ll \hat{J}_x$ . Therefore, we estimate that one needs of the order of  $\hat{J}_x/\epsilon$  powers of  $V$  to offset the energy  $\hat{J}_x$  required to flip a boundary spin. The probability corresponding to the required order of perturbation theory goes as  $[\|V\|]^{\hat{J}_x/\epsilon} \sim [\|V\|]^{J_x/O(J_z, g)}$  where  $\|V\|$  denotes the typical size of the matrix element that creates a domain wall. The above expression is a lower bound for the lifetime. For example, in the two integrable limits  $J_z \rightarrow 0, g \neq 0$  and  $g \rightarrow 0, J_z \neq 0$ , the lifetime should diverge. Empirically combining this observation with the rough estimate above we expect  $1/\epsilon = O(1/J_z, 1/g)$ . When  $J_z \ll g$  this empirical formula replaces  $\epsilon \rightarrow J_z$  in the above estimate making it consistent with Eq. (4).

**Conclusions:** ASPMs are fascinating objects which have lifetimes that far exceed bulk heating times. Besides presenting evidence for this, we developed a method for extracting their lifetimes by mapping their dynamics to single-particle quantum mechanics in Krylov subspace. An important direction of research is to derive how the lifetime depends on both  $g$  and  $J_z$ , and in the process improve on the domain wall counting argument.

*Acknowledgements:* This work was supported by the US Department of Energy, Office of Science, Basic Energy Sciences, under Award No. DE-SC0010821 (DJY and AM) and by the US National Science Foundation Grant NSF DMR-1606591 (AGA).

- 
- [1] T. Oka and S. Kitamura, Floquet engineering of quantum materials, *Annual Review of Condensed Matter Physics* **10**, 387 (2019), <https://doi.org/10.1146/annurev-conmatphys-031218-013423>.
  - [2] M. S. Rudner and N. H. Lindner, Band structure engineering and non-equilibrium dynamics in floquet topo-

- logical insulators, *Nat. Rev. Phys.* **2**, 229 (2020).
- [3] F. Harper, R. Roy, M. S. Rudner, and S. Sondhi, Topology and broken symmetry in floquet systems, *Annual Review of Condensed Matter Physics* **11**, 345 (2020).
- [4] S. Ryu, A. P. Schnyder, A. Furusaki, and A. W. W. Ludwig, Topological insulators and superconductors: tenfold



- way and dimensional hierarchy, *New Journal of Physics* **12**, 065010 (2010).
- [5] X.-L. Qi and S.-C. Zhang, Topological insulators and superconductors, *Rev. Mod. Phys.* **83**, 1057 (2011).
  - [6] B. A. Bernevig and (with T. L. Hughes), *Topological Insulator and Topological Superconductors*, Princeton University Press, Princeton (2013).
  - [7] D. Carpentier, P. Delplace, M. Fruchart, and K. Gawedzki, Topological index for periodically driven time-reversal invariant 2d systems, *Phys. Rev. Lett.* **114**, 106806 (2015).
  - [8] R. Roy and F. Harper, Abelian floquet symmetry-protected topological phases in one dimension, *Phys. Rev. B* **94**, 125105 (2016).
  - [9] R. Roy and F. Harper, Periodic table for floquet topological insulators, *Phys. Rev. B* **96**, 155118 (2017).
  - [10] M. S. Rudner, N. H. Lindner, E. Berg, and M. Levin, Anomalous edge states and the bulk-edge correspondence for periodically driven two-dimensional systems, *Phys. Rev. X* **3**, 031005 (2013).
  - [11] F. Nathan, M. S. Rudner, N. H. Lindner, E. Berg, and G. Refael, Quantized magnetization density in periodically driven systems, *Phys. Rev. Lett.* **119**, 186801 (2017).
  - [12] P. Titum, E. Berg, M. S. Rudner, G. Refael, and N. H. Lindner, Anomalous floquet-anderson insulator as a nonadiabatic quantized charge pump, *Phys. Rev. X* **6**, 021013 (2016).
  - [13] L. Jiang, T. Kitagawa, J. Alicea, A. R. Akhmerov, D. Pekker, G. Refael, J. I. Cirac, E. Demler, M. D. Lukin, and P. Zoller, Majorana fermions in equilibrium and in driven cold-atom quantum wires, *Phys. Rev. Lett.* **106**, 220402 (2011).
  - [14] M. Thakurathi, A. A. Patel, D. Sen, and A. Dutta, Floquet generation of majorana end modes and topological invariants, *Phys. Rev. B* **88**, 155133 (2013).
  - [15] J. K. Asbóth, B. Tarasinski, and P. Delplace, Chiral symmetry and bulk-boundary correspondence in periodically driven one-dimensional systems, *Phys. Rev. B* **90**, 125143 (2014).
  - [16] K. Sacha and J. Zakrzewski, Time crystals: a review, *Reports on Progress in Physics* **81**, 016401 (2017).
  - [17] D. V. Else, C. Monroe, C. Nayak, and N. Y. Yao, Discrete time crystals, *Annual Review of Condensed Matter Physics* **11**, 467 (2020).
  - [18] V. Khemani, R. Moessner, and S. Sondhi, A brief history of time crystals, *arXiv:1910.10745* (2019).
  - [19] V. Khemani, A. Lazarides, R. Moessner, and S. L. Sondhi, Phase structure of driven quantum systems, *Phys. Rev. Lett.* **116**, 250401 (2016).
  - [20] C. W. von Keyserlingk, V. Khemani, and S. L. Sondhi, Absolute stability and spatiotemporal long-range order in floquet systems, *Phys. Rev. B* **94**, 085112 (2016).
  - [21] C. W. von Keyserlingk and S. L. Sondhi, Phase structure of one-dimensional interacting floquet systems. i. abelian symmetry-protected topological phases, *Phys. Rev. B* **93**, 245145 (2016).
  - [22] C. W. von Keyserlingk and S. L. Sondhi, Phase structure of one-dimensional interacting floquet systems. ii. symmetry-broken phases, *Phys. Rev. B* **93**, 245146 (2016).
  - [23] V. M. Bastidas, C. Emary, G. Schaller, and T. Brandes, Nonequilibrium quantum phase transitions in the ising model, *Phys. Rev. A* **86**, 063627 (2012).
  - [24] D. J. Yates, F. H. L. Essler, and A. Mitra, Almost strong  $(0, \pi)$  edge modes in clean interacting one-dimensional floquet systems, *Phys. Rev. B* **99**, 205419 (2019).
  - [25] G. J. Sreejith, A. Lazarides, and R. Moessner, Parafermion chain with  $2\pi/k$  floquet edge modes, *Phys. Rev. B* **94**, 045127 (2016).
  - [26] D. A. Huse, R. Nandkishore, and V. Oganesyan, Phenomenology of fully many-body-localized systems, *Phys. Rev. B* **90**, 174202 (2014).
  - [27] Y. Bahri, R. Ronen, and E. Altman, Localization and topology protected quantum coherence at the edge of hot matter, *Nature Communications* **6**, 7341 (2015).
  - [28] D. V. Else, B. Bauer, and C. Nayak, Floquet time crystals, *Phys. Rev. Lett.* **117**, 090402 (2016).
  - [29] I.-D. Potirniche, A. C. Potter, M. Schleier-Smith, A. Vishwanath, and N. Y. Yao, Floquet symmetry-protected topological phases in cold-atom systems, *Phys. Rev. Lett.* **119**, 123601 (2017).
  - [30] A. Kumar, P. T. Dumitrescu, and A. C. Potter, String order parameters for one-dimensional floquet symmetry protected topological phases, *Phys. Rev. B* **97**, 224302 (2018).
  - [31] A. Y. Kitaev, Unpaired majorana fermions in quantum wires, *Physics-Uspekhi* **44**, 131 (2001).
  - [32] P. Fendley, Parafermionic edge zero modes in  $z_n$ -invariant spin chains, *Journal of Statistical Mechanics: Theory and Experiment* **2012**, P11020 (2012).
  - [33] A. S. Jermyn, R. S. K. Mong, J. Alicea, and P. Fendley, Stability of zero modes in parafermion chains, *Phys. Rev. B* **90**, 165106 (2014).
  - [34] P. Fendley, Strong zero modes and eigenstate phase transitions in the xyz/interacting majorana chain, *Journal of Physics A: Mathematical and Theoretical* **49**, 30LT01 (2016).
  - [35] D. V. Else, P. Fendley, J. Kemp, and C. Nayak, Prethermal strong zero modes and topological qubits, *Phys. Rev. X* **7**, 041062 (2017).
  - [36] J. Kemp, N. Y. Yao, C. R. Laumann, and P. Fendley, Long coherence times for edge spins, *Journal of Statistical Mechanics: Theory and Experiment* **2017**, 063105 (2017).
  - [37] D. E. Parker, R. Vasseur, and T. Scaffidi, Topologically protected long edge coherence times in symmetry-broken phases, *Phys. Rev. Lett.* **122**, 240605 (2019).
  - [38] J. Kemp, N. Y. Yao, and C. R. Laumann, Symmetry-enhanced boundary qubits at infinite temperature, *Phys. Rev. Lett.* **125**, 200506 (2020).
  - [39] D. J. Yates, A. G. Abanov, and A. Mitra, Lifetime of almost strong edge-mode operators in one-dimensional, interacting, symmetry protected topological phases, *Phys. Rev. Lett.* **124**, 206803 (2020).
  - [40] D. J. Yates, A. G. Abanov, and A. Mitra, Dynamics of almost strong edge modes in spin chains away from integrability, *Phys. Rev. B* **102**, 195419 (2020).
  - [41] V. Vishwanath and G. Müller, *The Recursion Method: Applications to Many-Body Dynamics*, Springer, New York (2008).
  - [42] H. Kim, T. N. Ikeda, and D. A. Huse, Testing whether all eigenstates obey the eigenstate thermalization hypothesis, *Phys. Rev. E* **90**, 052105 (2014).
  - [43] A. Lazarides, A. Das, and R. Moessner, Equilibrium states of generic quantum systems subject to periodic driving, *Phys. Rev. E* **90**, 012110 (2014).
  - [44] L. D'Alessio and M. Rigol, Long-time behavior of isolated

- periodically driven interacting lattice systems, *Phys. Rev. X* **4**, 041048 (2014).
- [45] P. Ponte, A. Chandran, Z. Papić, and D. A. Abanin, Periodically driven ergodic and many-body localized quantum systems, *Annals of Physics* **353**, 196 (2015).
  - [46] M. Bukov, M. Heyl, D. A. Huse, and A. Polkovnikov, Heating and many-body resonances in a periodically driven two-band system, *Phys. Rev. B* **93**, 155132 (2016).
  - [47] A. Haldar, R. Moessner, and A. Das, Onset of floquet thermalization, *Phys. Rev. B* **97**, 245122 (2018).
  - [48] D. E. Parker, X. Cao, A. Avdoshkin, T. Scaffidi, and E. Altman, A universal operator growth hypothesis, *Phys. Rev. X* **9**, 041017 (2019).
  - [49] A. Dymarsky and A. Gorsky, Quantum chaos as delocalization in krylov space, *Phys. Rev. B* **102**, 085137 (2020).
  - [50] J. Barbón, E. Rabinovici, R. Shir, and R. Sinha, On the evolution of operator complexity beyond scrambling, *Journal of High Energy Physics* **2019**, 264 (2019).
  - [51] A. Avdoshkin and A. Dymarsky, Euclidean operator growth and quantum chaos, *Phys. Rev. Research* **2**, 043234 (2020).
  - [52] W. E. Arnoldi, The principle of minimized iterations in the solution of the matrix eigenvalue problem, *Quart. Appl. Math.* **9**, 17 (1951).
  - [53] D. V. Else, B. Bauer, and C. Nayak, Prethermal phases of matter protected by time-translation symmetry, *Phys. Rev. X* **7**, 011026 (2017).
  - [54] D. A. Abanin, W. De Roeck, and F. Huveneers, Exponentially slow heating in periodically driven many-body systems, *Phys. Rev. Lett.* **115**, 256803 (2015).
  - [55] T. Kuwahara, T. Mori, and K. Saito, Floquet–magnus theory and generic transient dynamics in periodically driven many-body quantum systems, *Annals of Physics* **367**, 96 (2016).
  - [56] T. Mori, T. Kuwahara, and K. Saito, Rigorous bound on energy absorption and generic relaxation in periodically driven quantum systems, *Phys. Rev. Lett.* **116**, 120401 (2016).
  - [57] D. A. Abanin, W. De Roeck, W. W. Ho, and F. Huveneers, Effective hamiltonians, prethermalization, and slow energy absorption in periodically driven many-body systems, *Phys. Rev. B* **95**, 014112 (2017).
  - [58] D. Abanin, W. De Roeck, W. W. Ho, and F. Huveneers, A rigorous theory of many-body prethermalization for periodically driven and closed quantum systems, *Communications in Mathematical Physics* **354**, 809 (2017).
  - [59] A. Eckardt and E. Anisimovas, High-frequency approximation for periodically driven quantum systems from a floquet-space perspective, *New Journal of Physics* **17**, 093039 (2015).
  - [60] R. Scharf, The campbell-baker-hausdorff expansion for classical and quantum kicked dynamics, *Journal of Physics A: Mathematical and General* **21**, 2007 (1988).
  - [61] L. D’Alessio and A. Polkovnikov, Many-body energy localization transition in periodically driven systems, *Annals of Physics* **333**, 19 (2013).